Available online at www.sciencedirect.com
SCIENCE DIRECT®
Computational Materials Science 36 (2006) 319–328
COMPUTATIONAL MATERIALS SCIENCE
www.elsevier.com/locate/commatsci

Computer simulations of true stress development and viscoelastic behavior in amorphous polymeric materials

Ricardo Simões [a,b,*], António M. Cunha [a], Witold Brostow [b]

[a] Institute for Polymers and Composites (IPC), Department of Polymer Engineering, University of Minho, 4800-058 Guimarães, Portugal
[b] Laboratory of Advanced Polymers and Optimized Materials (LAPOM), Department of Materials Science and Engineering, University of North Texas, Denton, TX 76203-5310, USA

Received 7 March 2005; received in revised form 4 April 2005; accepted 12 April 2005

Abstract

Molecular dynamics simulations were employed to study the mechanical properties and true stress development in amorphous polymeric materials. As expected, the true stress levels are much higher than those indicated by the engineering stress. However, the true stress behavior was found to be not only *quantitatively* but also *qualitatively* different from that of the engineering stress. Highly localized deformation results in abrupt increases of the true stress in certain regions, favoring crack formation and propagation. The computer-generated materials exhibit viscoelastic recovery curves similar to those seen in experiments. The recovery process is non-homogeneous and affected by the spatial arrangement of the amorphous chains. The loading conditions determine the preferential deformation mechanisms and influence the extent of recovery. Some deformation mechanisms are *not* recovered and contribute to permanent deformation.

PACS: 07.05.T; 36.20.E; 36.20.F; 62.20.F

Keywords: Computer simulations; Molecular dynamics; Polymer viscoelasticity; True stress; Mechanical properties; Structure–properties relationships

1. Introduction

As argued before, service performance and reliability of polymeric materials are of interest to all, not only to scientists and engineers [1,2]. As polymers become more widely used and in many demanding applications are replacing metals and ceramics, understanding their behavior becomes a critical issue. However, the properties of polymers are often difficult to characterize and even more difficult to predict, due to their complex structure and to the variety of factors involved, namely the time-dependent behavior, the processing history and their anisotropic character.

Computer simulations have an enormous potential to provide better understanding of the behavior and properties of polymeric materials. As eloquently argued by Fossey [3], simulations provide information not readily accessible experimentally; this either due to the prohibitively difficult nature of the tests, the inadequacy of existing equipment and techniques to study a particular phenomena, or other impediments. A significant advantage of computer simulations is the ability to create

* Corresponding author. Address: Institute for Polymers and Composites (IPC), Department of Polymer Engineering, University of Minho, 4800-058 Guimarães, Portugal. Tel.: +351 253510320; fax: +351 253510339.
E-mail addresses: rsimoes@dep.uminho.pt (R. Simões), amcunha@dep.uminho.pt (A.M. Cunha), brostow@unt.edu (W. Brostow).

0927-0256/$ - see front matter © 2005 Elsevier B.V. All rights reserved.
doi:10.1016/j.commatsci.2005.04.007

conditions that cannot be replicated in a controlled experimental environment. Even more importantly, they can be used to determine the effects of one system variable at a time.

As pointed out by Gilman [4], not all computer simulations are of interest, particularly those which only confirm what is already known from experiments. This paper meets this challenge, introducing a method for the determination of true stress response of computer-generated materials (CGMs). Results on viscoelastic behavior of simulated amorphous polymers are also reported.

It is important to point out that the simulations presented and discussed in this paper were *not* performed with the intent of replacing experiments but rather to complement them. The concomitant use of computer simulations and experiments should produce a synergistic effect, enabling a more complete understanding of the properties and behavior of polymeric materials.

2. Applications of computer simulations to polymer behavior and properties

At least three simulation approaches have been widely used by the scientific community: the Monte Carlo (MC), the Brownian dynamics (BD), and the molecular dynamics (MD) methods [5,6]. MD is the method preferred by our research group for the present purpose of studying the time-dependent deformation of polymeric materials. This method was originally developed by Alder and Wainwright, with the intent of determination of phase diagrams of systems of hard spheres [7]. At a later stage, continuous potentials allowed a more realistic response of the system. Rahman was the first to introduce Mie potentials (often called Lennard-Jones potentials) in the MD simulations [8], which created the basis for most of the work done in this area since then.

Atomistic simulations have been extensively used to study molecular-level phenomena in polymers [9–12]. Termonia and Smith have used the kinetic model of fracture to simulate the mechanical behavior of polymers [13–15] and spider silk fibers [16]. Fossey and Tripathy [17] have also dealt with this topic, having combined the method of Theorodou and Suter [10] to form a polypeptide glass with Termonia's spider silk elasticity three-phase system model.

A different approach to the mechanics of polymers consists in the use of linear and non-linear fracture mechanics [18–20], including the essential work of fracture (EWF) method. An extensive review on fracture mechanics approaches used to describe the behavior of polymers has been provided by Nishioka [21]. Binienda and co-workers have also employed such methods in the analysis of crack development [22,23].

Bicerano has employed numerical simulations and the Monte Carlo method to simulated stress–strain curves of rubbery amorphous and semi-crystalline polymers [24], where the amorphous rubbery phase exhibits both chemical crosslinks and physical entanglements. He had previously proposed a model for studying dynamic relaxations in amorphous polymers [25].

A review paper on both continuum mechanics and molecular models for describing yield in amorphous polymers has been provided by Stachurski [26], including a discussion on computer modeling results from different authors in view of molecular deformation and yield theories. In more recent work the same author employs micro-mechanics theories to model deformation mechanisms in amorphous polymers, obtaining simulated stress vs strain curves in qualitative agreement with experimental data [27].

The MD method is widely used for simulations of material systems, and can be applied from the atomistic level to the mesoscale. One of its major advantages over alternative methods is the use of time as an explicit variable, allowing for simulation of both equilibrium properties and time-dependent ones—an essential feature for simulation of viscoelastic materials. The MD method considers a system of N particles (statistical chain segments in this case), each described by three Cartesian coordinates and three momentum components along the main axes. In order to obtain the time-dependent behavior of the system, these six variables are calculated at every time step of the simulation. Typically, the status of the system is analyzed every several thousand time steps (every 2000 time steps in the simulations reported here).

MD methods have been used to study a wide variety of phenomena, in many different fields of work. Smith et al. [28] used MD to simulate the X-ray scattering pattern. Gerde and Marder [29] investigated friction and its connection to the mechanism of self-healing cracks. Theodorou et al. have investigated the phenomena of diffusion [30], permeation [31], elongational flow [32], and stress relaxation [33]. However, they have performed their simulations mostly at the atomistic level, following a different approach from the one employed in the present study. Other relevant MD simulations applied to materials science include the thermodynamic properties of simple fluids and polymer melts [34,35], the melting phenomena including that of thin layers on a substrate [36,37], and transport of fluids through polymer membranes [38].

Simulations of stress relaxation in metals and polymers have been previously reported [39,40]. The presence of defects was found to greatly affect the response, increasing by several orders of magnitude the time span for relaxation. These simulations have shown also that stress relaxation is mainly achieved by plastic deformation in the vicinity of defects. A higher

force is required to initiate a crack in an ideal lattice, but then the force is sufficient to cause quick propagation. The simulated stress–relaxation curves mimic all the essential features of experimental curves and also are in accordance with the Kubát cooperative theory of stress relaxation in materials [41].

More recently, computer simulations were employed in the study of mechanical properties [5] and the crack formation and propagation phenomena in polymer liquid crystals (PLCs) [42]. This works goes in parallel with our predictions of long term behavior of PLCs from short term tests [2] and also using statistical mechanics to determine PLC behavior [43,44]. One of the key questions is where cracks form in the material and how they propagate through it. The cracks can be equally expected to form in the flexible matrix because of its relative weakness or inside the reinforcing phase because of its relative rigidity. The simulations results have indicated that cracks appear preferentially between second phase agglomerates in close proximity, growing next to the interface between the two phases. Cracks can then propagate through the flexible phase, including connecting to other cracks.

A similar approach was also developed to perform the first simulations of scratching in amorphous materials [45]. The results show how local structure affects scratch resistance and recovery; preferential migration of a rigid second phase to the surface of a two-phase material can improve its tribological performance.

State-of-the-art in computer simulations of polymeric materials includes the work by Grest on poly(dimethylsiloxane) [46,47], which exhibits excellent agreement with X-ray scattering measurements. Grest and Plimpton have also investigated several methods for the equilibration of long chain polymer melts [48]. Rottler and Robbins have studied shear yielding in glassy polymers under triaxial loading [49], as well as the growth and failure of crazes in amorphous glassy polymers [50,51].

3. Simulation method

The model used for simulation considers a polymeric chain as a set of statistical segments (or "beads"), where each statistical segment represents several repeating units of the material. This model, advocated by Flory [52], allows for simulations at larger scale than those using the united-atom model or those performed at the atomistic level. The statistical segment model is also often named *coarse grain* model. Section 4 covers the procedure for creating the materials on the computer.

Each of the segments interacts with its neighbors through pair-wise interactions. These are described by a set of interaction potentials that differ for primary (intra-chain) and secondary (inter-chain) bonds. A spliced double well potential characterizes the strong primary bonds, allowing for conformation transitions as in real polymer chains. A much weaker Morse-like potential is used for the secondary interactions. A detailed description of the interaction potentials has been previously provided [5].

The molecular dynamics (MD) method was used to simulate the time-dependent behavior of the system, with the time evolution calculated through a leap-frog algorithm [53]. The advantages over other simulation methods have been discussed before [5,42].

The employed MD simulation method assumes that the forces on particles are nearly constant over very short time periods—what defines the time step for the simulation. The value of the time step was previously discussed [40], together with a detailed description of the time integration method. It can be shown that in the limit of short time steps, this procedure samples states accessible in the micro-canonical ensemble. However, additional features can be added to the algorithm that allow one to specify the configurational temperature, or allow the simulation to access a range of energies and/or pressures that correspond to either the canonical or isothermal-isobaric ensembles.

When using the micro-canonical ensemble, one maintains the number of particles, volume and energy (NVE) constant throughout the simulation. However, the simulations reported in this paper were performed at constant temperature (room temperature) to avoid an effect of stochastic thermal forces; this because the purpose is to study non-thermal sources of polymer fracture [40]. Also, the material is allowed to deform freely along all three axes. This implies that upon sufficient deformation, there is formation and propagation of cracks, resulting in an increase of the internal free volume. Thus, this procedure is closer to the isothermal ensemble. When performing constant-temperature MD [53], one has to rescale the velocities at each time step, based on the kinetic energy of the system. Further details concerning the simulation model were previously provided [5,40].

4. Material generation procedures

In order to perform the simulations, one must first create a polymeric material on the computer. Although previous work reported results pertaining to two-phase polymer liquid crystals, the present paper deals with single-phase amorphous polymers.

The approach used to create the chains was initially developed by Mom [54] and later modified [55]. The method results in a system of self-avoiding chains on a three-dimensional lattice. In previous 2D simulations, the triangular lattice had been chosen for several reasons stated before [39,55]. Particularly, this lattice results in a

more realistic coordination number than, for example, the square lattice. Likewise, for the present 3D simulations the hexagonal close packed lattice was chosen over the cubic lattice. The methodology is effective both for completely filled lattices and those containing vacancies.

Initially, all segments in the material are positioned at equidistant lattice locations, each segment representing at this stage one chain of length 1. The system is then searched for neighboring end-of-chain segments. At the first stage, all segments fulfill this condition and therefore a statistical function determines which segments bond together forming chains of length 2. The chains continue to grow by bonding of adjacent end-of-chain segments until no more segments can be bonded in this way. When a segment can equally bond to several others, the choice of which two segments to connect is made at random.

While the procedure appears simple, the resulting materials exhibit realistic features, such as a molecular weight distribution and physical entanglements between chains [55].

Two optimization algorithms can also be used in order to increase the average molecular weight of the chains and simultaneously introduce vacancies in the material. These algorithms are based on the removal of specific end-of-chain segments in order to allow new bonds to be created.

A detailed description of the entire one- and two-phase material generation procedure, including a brief review of alternative methods to generate polymeric materials on a computer, has been provided elsewhere [55].

5. Simulation details

As noted in Section 1, obtaining *true stress* values is an important objective. As discussed in textbooks of Materials Science and Engineering (MSE), uniaxial extension constitutes the most widely used mechanical test [56]. During that extension the minimal cross-sectional A_m area of the specimen decreases. However, one uses the initial cross-sectional area A_0 determined before application of the tensile force F. Thus, instead of the true stress $\sigma_t = F/A_m$ one works with the *engineering stress* $\sigma_n = F/A_0$. The failure of the specimen occurs earlier than the engineering stress values would suggest. As the present simulations have the capability to evaluate both kinds of stress, the dependence of both parameters on time is presented below and the differences between them discussed.

A specific procedure for the evaluation of changes of A_m with time during the simulations was developed. The computer-generated tensile specimen is divided into a number of sections; 10 is a convenient number—although it could easily be changed to accommodate materials of larger sizes or of complicated shapes. The geometry of each section is monitored with time and thus the true stress calculated and updated for each section. By definition, the highest value of σ_t found in any section is the true stress in the specimen. In experiments, deformation is non-homogeneous, with a localized necking and crack formation taking place. Similar behavior is expected from the simulations, with significant changes in the true stress with time.

During the simulation, a uniaxial external tensile force is applied to the edges of the material along the x-axis. Simulations can be performed with the value of the external force increasing continuously until fracture of the material is observed. Another option consists in the force removal after a stipulated number of steps and monitoring of the subsequent viscoelastic recovery. Recovery, well known in polymer mechanics, has been found also in tribology: significant shallowing of the scratch depth with time, this both in experiments [57,58] and in simulations [45].

Before the simulation begins, the segments are perturbed from their initial lattice positions by a random small fraction (between 1/100 and 1/1000) of the average intersegmental distance. This perturbation from the ideal lattice positions is sufficient to originate a starting configuration appropriate for the off-lattice simulation, but without inducing exaggerated attractive or repulsive forces during the first simulation steps.

At the first stage of the simulation the material is allowed to equilibrate for 2000 time steps without any external forces applied. The 2000 equilibration time steps were found sufficient for the simulated materials to recover from the induced perturbation mentioned before, after which every segment is merely oscillating around the equilibrium distance. After this quasi-equilibrium state has been reached, an external force is imposed and the state of the system is monitored and periodically recorded [5]. The external tensile force is applied to all segments on both edges of the material along the x-axis (see Fig. 1a).

Since the force is always applied along the x-axis, the cross-section is defined in the y–z plane. All sections are initially parallelepipeds of equal size, except for the section number 10 (the last one) which will be created based on the exact number of columns in the material. Each section is defined by the positions of the segments at their eight corners. These segments are assigned to each section in the beginning of the simulation; their changes in position along time determine the geometry of the sections. The initial division of the material in sections and the definition of a section are shown in Fig. 1.

Each section can be characterized by two cross-sectional areas, one defined by the leftmost segments and the other defined by the rightmost segments along the x-axis. These two areas are labeled A_l and A_r in Fig. 1b, and are simply called the left area and right area

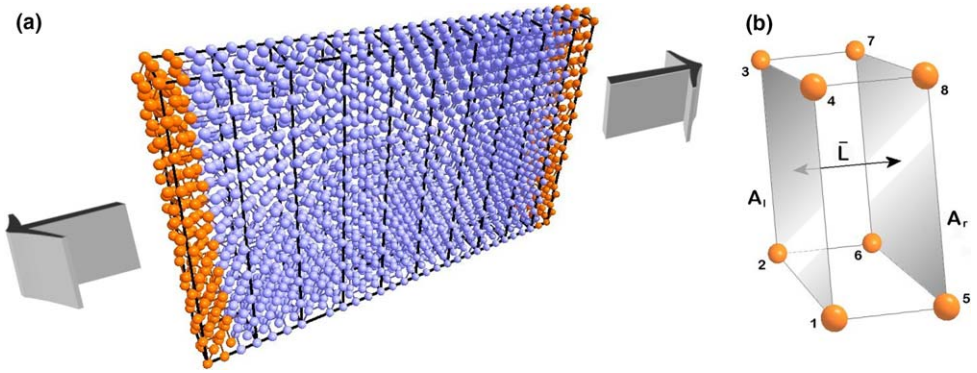

Fig. 1. (a) Initial shape of one of the simulated computer-generated materials (CGMs); the external force is applied to the leftmost and rightmost edge segments along the x-axis. (b) Definition of a section in a CGM.

of the section. The average distance between these two areas provides an average value of the length of the individual section $\overline{L}$. The average cross-sectional area $\overline{A}$ is calculated for each section simply as the average of A_l and A_r. The volume of the section V can be approximated as the average section area multiplied by the average length of the section. The free volume V_f is then calculated as the section volume minus the volume occupied by all segments inside the box defined by the eight corners of the section. The equations used for calculating variables related with the sections are:

$$A_l = \left[\frac{(y_3 + y_4) - (y_1 + y_2)}{2}\right] \times \left[\frac{(z_3 + z_2) - (z_1 + z_4)}{2}\right] \tag{1}$$

$$A_r = \left[\frac{(y_7 + y_8) - (y_5 + y_6)}{2}\right] \times \left[\frac{(z_7 + z_6) - (z_5 + z_8)}{2}\right] \tag{2}$$

$$\overline{A} = \frac{A_l + A_r}{2} \tag{3}$$

$$\overline{L} = \frac{\sum_{i=5}^{8} x_i - \sum_{i=1}^{4} x_i}{4} \tag{4}$$

$$V = \overline{A} \times \overline{L} \tag{5}$$

$$V_f = V - I \times V_0 \tag{6}$$

Here, x_i, y_i and z_i are respectively the x-coordinate, y-coordinate and z-coordinate of corner i, V_0 is the volume of an individual segment (volume of a sphere of radius 0.5), and I is the number of segments inside the section.

As the material deforms under an applied force, the geometry of the sections is monitored and used to calculate the true stress levels. Fig. 2 shows the section geometry change in a sample material at a certain instant during a simulation of uniaxial deformation. The true stress σ_t is calculated based on the minimum average cross-sectional area of all sections:

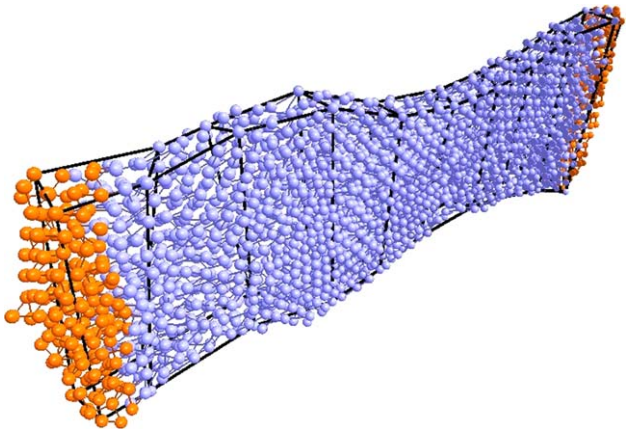

Fig. 2. Changes in the geometry of the CGM sections during tensile deformation.

$$\sigma_t = \frac{F_{ext}}{\min\left\{\overline{A}_1, \overline{A}_2, \ldots, \overline{A}_{10}\right\}} \tag{7}$$

There are some unavoidable approximations involved in this analysis: (a) segments intersected by the boundary between two sections are considered as belonging to only one of them; (b) a few segments sometimes escape the overall boundaries of all sections. These effects have been thoroughly tested and found to have negligible effects on the final results. However, when the system reaches large-scale deformation, the shape of the sections sometimes becomes inadequate for calculating the cross-sectional area. In this case, the user must determine up to which simulation step the values of the true stress should be considered.

Since this work deals with phenomena at a molecular level, one might argue with applying the general concept of macroscopic strain at this scale. However, by employing again the sections concept, the strain is calculated from the distance between the leftmost and rightmost average cross-sectional areas of the material, that is, A_l of section 1 and A_r of section 10. Although typically one would be interested in measuring the strain at break

as a material property, the random nature of the cracking phenomena makes it more useful in some cases to measure the strain at a certain time into the simulation. Since all simulations are performed with the same loading conditions, that measurement is representative of the mechanical history of the sample and of the material response.

A single simulation was run for each set of conditions. This was mainly imposed by the computation time required for each simulation. The variability of results from several simulations with the same set of conditions was confirmed to be small enough not to affect the overall results discussed in this paper.

Note that in the results discussed below the time scale is in simulation steps since the status of the material is not recorded every time step, but only every 2000 time steps. Thus, each simulation step corresponds to 2000 time steps.

6. Selected results

6.1. True stress vs nominal stress

In 3D materials of coiled chains, one can define a cross-sectional area and monitor its changes during deformation. As described above in Section 5, that information can be used to calculate the true stress level in the material and also changes in free volume during deformation. The true stress can then be compared with the engineering stress.

For this purpose, a fully flexible computer generated material (CGM) within a simulation cell containing approximately 1800 statistical segments has been simulated under an external tensile force increasing at a constant rate. In average there are 40–50 macromolecular chains in each CGM. The chosen size of the simulation cell was dictated by the available computational resources in order to perform these simulations in a reasonable time. The effect of the system size on the response was verified for several similar CGMs. Within the studied range, materials with different sizes still exhibit the same tendencies and properties described in this paper. The engineering and true stress levels during deformation of the material are shown in Fig. 3.

Fig. 3 shows true stress values considerably higher than those of the engineering stress. Clearly, this is due to a decrease of the cross-sectional area that accompanies deformation. Moreover, the true stress increases irregularly; the deformation mechanisms and the formation of micro-cracks are not continuous processes at the molecular level, as shown before [59].

Considering the same material under different loading conditions, with the force increasing at a constant rate for 15 simulation steps and then kept constant until fracture is observed, the engineering stress exhibits the same pattern as the force and it would appear that the material is under a constant stress value after simulation step 16; see Fig. 4. However, as shown also in Fig. 4, the true stress level continues to increase up to fracture. The cross-sectional area is changing significantly during the simulation.

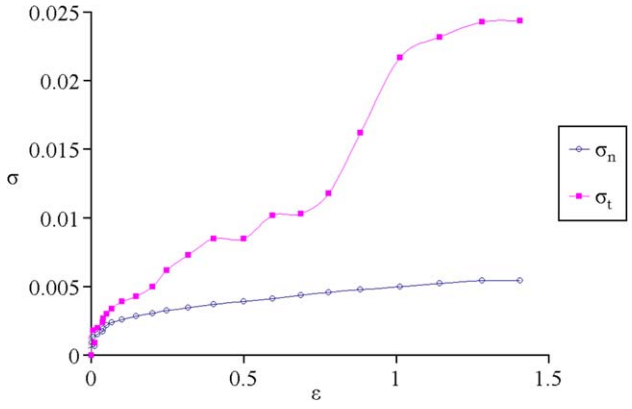

Fig. 3. Evolution of the engineering stress (σ_n) and true stress (σ_t) levels during the simulation of a fully flexible material under an external force increasing up to fracture. Here, ε is the strain.

6.2. Strain behavior

The evolution of the strain and the free volume along the simulation can also be compared; see Fig. 5.

The strain begins to increase only after several simulation steps—when the force is sufficient for deformation mechanisms to take place. However, during the first deformation stage, the slope of the strain curve is low. This corresponds to the mechanisms requiring lower force values. Since the force increases continuously, the slope of the strain curve changes at around 13 simulation steps; from that point on, the strain rapidly increases up to fracture.

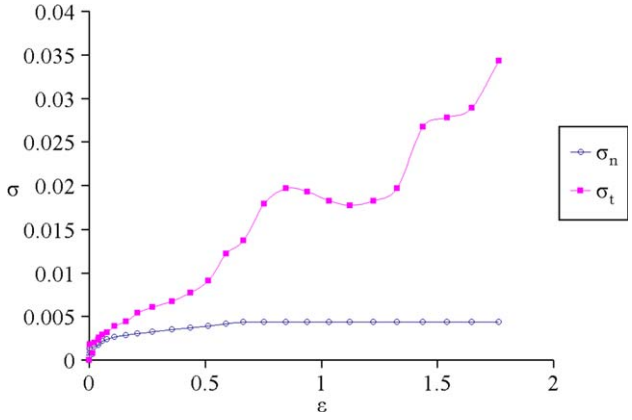

Fig. 4. Evolution of the engineering stress (σ_n) and true stress levels (σ_t) during the simulation of a fully flexible material under an external force. The applied force increases for the first 15 simulation steps and then remains constant up to fracture. Here, ε is the strain.

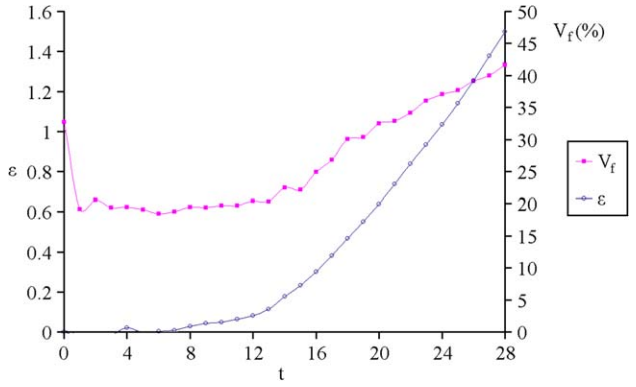

Fig. 5. Evolution of the strain (ε) and the free volume (V_f) during simulation. Here, t is the number of simulation steps.

The free volume curve provides additional information. After the initial random perturbation from the ideal lattice positions, the material has approximately 33% free volume. The drop in free volume to approximately 20% after the first simulation step corresponds to the equilibration of the material. These values are not far from 26% for the ideal lattice, which indicates an acceptable representation of the material geometry by the defined sections. The free volume remains approximately constant for 10 simulation steps, even though the material is being strained. Apparently the deformation is occurring at *nearly constant volume*, with a decrease in the cross-section accompanying elongation along the force application direction.

After this point, the free volume starts increasing and continues to do so up to fracture. This implies the formation and propagation of cracks inside the material. The free volume in Fig. 5 is calculated as the average value for the ten sections. However, the free volume does not change uniformly throughout the material. To verify this, the free volume for each section along time is represented in Fig. 6. Recall that relatively small amounts of free volume enhance the chain relaxation capability (CRC) [2,60]. Apparently large V_f values calculated according to this procedure are indicative of cracks.

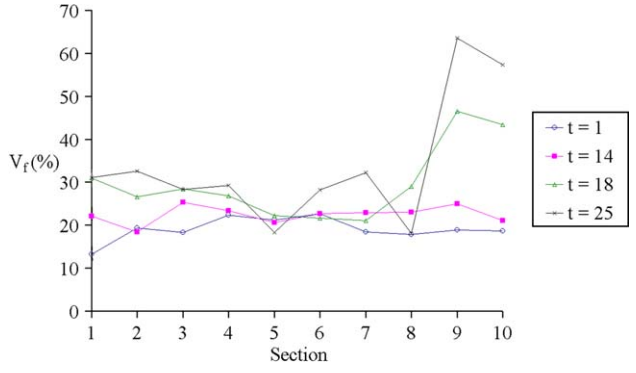

Fig. 6. Changes in the free volume (V_f) of individual sections during simulation. The lines connecting the values were represented only for better visualization. Here, t is the number of simulation steps.

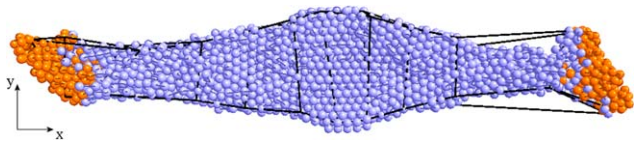

Fig. 7. Geometry of the material near the moment of fracture.

Clearly, in the late stages of the simulation the free volume increases significantly for sections 9 and 10, while some sections still exhibit values nearly unchanged since the beginning of the simulation. The material actually fractures around sections 9 and 10, as shown in Fig. 7 as anticipated by high values of the free volume. It is also important to note that near fracture the cross-sectional area should tend to zero, causing the true stress to tend to infinity. However, since the true stress is calculated from the geometry of the sections, the effect is somewhat masked.

6.3. Viscoelastic recovery

It is also interesting to observe the material response when the force is applied for a certain period and then removed. This will validate the viscoelastic nature of the model and simultaneously allow the study of the material behavior during recovery.

Considering again the material studied in Sections 6.1 and 6.2, an external force increasing at the constant rate of 0.01 was applied for 20 simulation steps and then removed. The recovery of the material after force removal was monitored for 30 additional simulation steps. The strain behavior and the changes in free volume during the simulation are shown in Fig. 8.

As expected, the strain increases up to the point of force removal. The material then recovers, and two stages of this process can be distinguished. The strain decreases rapidly for about 7 simulation steps and then slowly for another 22 simulation steps. The strain

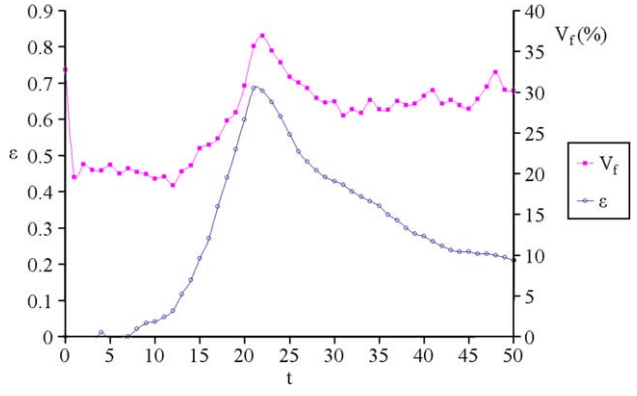

Fig. 8. Deformation and subsequent viscoelastic recovery after force removal are evident in the behavior of the strain (ε) and free volume (V_f) curves. Here, t is the number of simulation steps.

decreases approximately 35% of the maximum value in each of those two stages. After this point, the recovery is very small and thus one can consider that the material has reached a meta-stable state.

The free volume curve in Fig. 8 provides additional information regarding deformation. After an initial stage during which the free volume remains almost unchanged, it then increases together with the rapid increase of the strain up to force removal. Similarly to the strain, V_f then decreases for several simulation steps, but eventually stabilizes and does not decrease continuously as the strain does. This is due to the material buckling instead of recovering to the initial shape. It is important to note how the peaks of the strain and free volume occur at the same time; the same does not occur for strain and stress, as will be presented in a separate paper.

The structure of the material is represented at different stages of the simulation in Fig. 9.

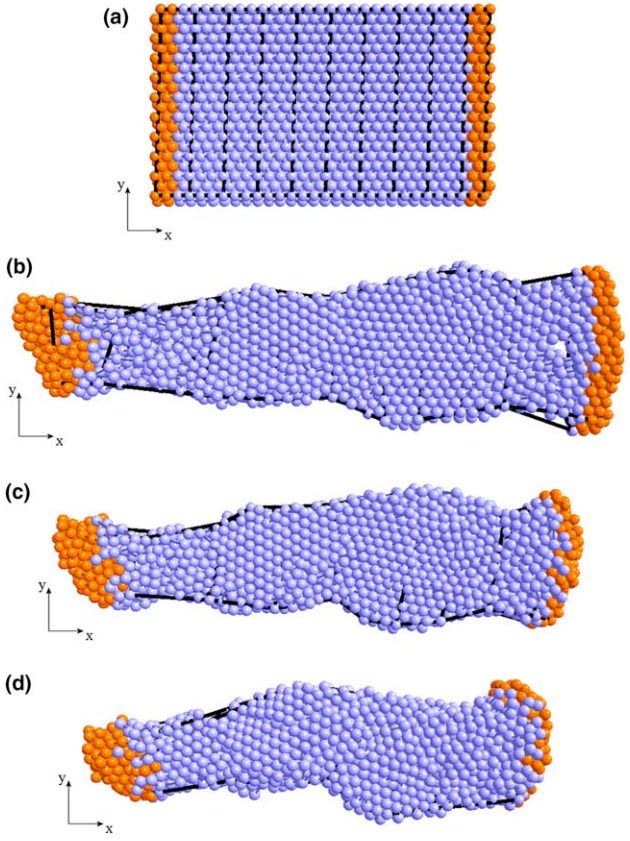

Fig. 9. (a) Geometry of the material at time $t = 1$ simulation step, the beginning of the tensile simulation. Until this moment, no external force has been applied. (b) Geometry of the material at time $t = 21$ simulation steps, immediately before force removal. This corresponds to the maximum strain observed. (c) Geometry of the material at time $t = 28$ simulation steps. Some recovery has been observed in a few steps without external forces applied. (d) Geometry of the material at time $t = 50$ simulation steps. Over an extended period without external forces applied, a significant amount of deformation was recovered.

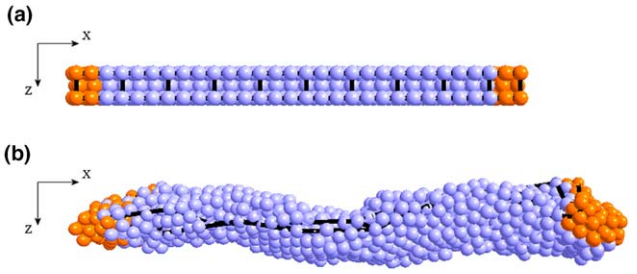

Fig. 10. (a) Initial geometry of the material viewed from the top; (b) geometry of the material at time $t = 50$ simulation steps viewed from the top. A considerable expansion along the z-axis is observed during the recovery stage.

The recovery of the material is not uniform; the final shape is very different from the initial one; see again Fig. 9d. This is due to the force only having been removed after significant deformation occurred; in fact, the force has been removed at a point quite close to fracture. For very small deformations, the material can recover to a shape closely resembling the initial state.

Another important observation is associated to the free motion of the material along any axis and its tendency to buckle and expand along the z-axis during recovery. In some cases, the length along the x-axis even becomes smaller than the initial value, which would indicate unreasonable negative contraction. However, by analyzing the free volume curves and graphically visualizing the simulation results, one can confirm that the material is simply expanding along the z-axis. Fig. 10 shows the initial and final structure of the material seen from the top.

7. Concluding remarks

By calculating the true stress on the material, one can observe how the changes in cross-sectional area result in stress levels much higher than those indicated by the engineering stress. This procedure provides a much more realistic measure of the true mechanical state imposed on the material. The true stress behavior was found to be not only *quantitatively* but also *qualitatively* different from that of the engineering stress. Moreover, since the material often exhibits highly localized deformation, the true stress in a certain region can increase substantially compared to the overall values. In that case, those regions become probable *loci* for failure to occur. This effect is also reflected in the free volume values for those regions. On one hand, the free volume affects the mobility of the segments via CRC. On the other hand, large *local* amounts of free volume provide an opportunity for crack formation and propagation.

By simultaneously analyzing the strain and free volume curves, detailed information about the deformation

mechanisms is obtained. First, short-scale deformation was found to be achieved at near-constant free volume; as the material elongates in the direction of force application, the average cross-section is decreasing. When significant increases in V_f occur under larger deformations, they reflect the fact that cracks begin to appear and grow. These results corroborate what had been stated before about deformation mechanisms taking place at the mesoscale in polymeric materials [59]. This previous publication includes several animations of the tensile deformation of these materials.

When a force is applied and then removed after large-scale deformation has occurred, the CGMs exhibit viscoelastic recovery. A significant part of the imposed deformation is recovered, but after some time the recovery reaches a *plateau*. The recovery process is non-homogeneous and depends on the chain structure of the material. Deformation mechanisms such as chain slippage and bond rupture are *not* recovered and contribute to permanent deformation. The CGMs have a tendency to buckle during recovery; this phenomenon will be further investigated in future work.

A better understanding of the molecular phenomena that take place during deformation of polymers emerges from these simulations. The possibility of predicting the mechanical properties from simulation results is encouraging. However, further work is warranted, particularly so on connections between the nano- and mesoscopic levels and macroscopic properties and behavior.

Acknowledgements

Support for this research has been provided by the Fundação para a Ciência e a Tecnologia, Lisbon, through the 3° Quadro Comunitário de Apoio, and through the POCTI and FEDER programmes, and also by the Robert A. Welch Foundation, Houston (Grant # B-1203). The authors also acknowledge discussions with Prof. J. Karger-Kocsis, University of Kaiserslautern.

References

[1] W. Brostow, R.D. Corneliussen (Eds.), Failure of Plastics, Hanser, Munich–Vienna–New York, 1992.
[2] W. Brostow, N.A. D'Souza, J. Kubát, R.D. Maksimov, J. Chem. Phys. 110 (1999) 9706.
[3] S. Fossey, in: W. Brostow (Ed.), Performance of Plastics, Hanser, Munich–Cincinnati, 2000, p. 63.
[4] J.J. Gilman, Mater. Res. Innovat. 4 (2001) 209.
[5] W. Brostow, M. Donahue III, C.E. Karashin, R. Simoes, Mater. Res. Innovat. 4 (2001) 75.
[6] W. Brostow, M. Drewniak, J. Chem. Phys. 105 (1996) 7135.
[7] B.J. Alder, T.E. Wainwright, J. Chem. Phys. 27 (1957) 1208.
[8] A. Rahman, Phys. Rev. A 136 (1964) 405.
[9] G.C. Rutledge, U.W. Suter, Macromolecules 24 (1991) 1921.
[10] D.N. Theodorou, U.W. Suter, Macromolecules 19 (1986) 139.
[11] M. Parrinello, A. Rahman, J. Chem. Phys. 76 (1982) 2662.
[12] D.R. Rottach, P.A. Tillman, J.D. McCoy, S.J. Plimpton, J.G. Curro, J. Chem. Phys. 111 (1999) 9822.
[13] Y. Termonia, in: Encyclopedia of Polymer Science and Technology, third ed., Wiley-Interscience, New York, 2002.
[14] Y. Termonia, P. Smith, Macromolecules 20 (1987) 835.
[15] Y. Termonia, P. Smith, Macromolecules 21 (1988) 2184.
[16] Y. Termonia, Macromolecules 27 (1994) 7378.
[17] S. Fossey, S. Tripathy, Int. J. Biol. Macromol. 24 (1999) 119.
[18] J. Karger-Kocsis, in: A.M. Cunha, S. Fakirov (Eds.), Structure Development During Polymer Processing, Kluwer, Dordrecht, 2000, p. 163.
[19] J. Karger-Kocsis, in: J.G. Williams, A. Pavan (Eds.), Fracture of Polymers, Composites and Adhesives, ESIS vol. 27, Elsevier Science, Oxford, 2000, p. 213.
[20] O.O. Santana, M.L. Maspoch, A.B. Martinez, Polym. Bull. 39 (1999) 511.
[21] T. Nishioka, Int. J. Fract. 86 (1997) 127.
[22] Y. Li, H. Ann, W.K. Binienda, Int. J. Solids Struct. 11 (1998) 981.
[23] N. Shbeeb, W.K. Binienda, K. Kreider, Int. J. Fract. 104 (2000) 23.
[24] J. Bicerano, N.K. Grant, J.T. Seitz, K. Pant, J. Appl. Polym. Sci. Part B: Polym. Phys. 35 (1997) 2715.
[25] J. Bicerano, J. Appl. Polym. Sci. Part B: Polym. Phys. 29 (1991) 1329.
[26] Z.H. Stachurski, Prog. Polym. Sci. 22 (1997) 407.
[27] Z.H. Stachurski, Polymer 44 (2003) 6067.
[28] C. Ayyagari, D. Bedrov, G.D. Smith, Macromolecules 33 (2000) 6194.
[29] E. Gerde, M. Marder, Nature 413 (2001) 285.
[30] N.C. Karayiannis, V.G. Mavrantzas, D.N. Theodorou, Chem. Eng. Sci. 56 (2001) 2789.
[31] K. Makrodimitris, G.K. Papadopoulos, D.N. Theodorou, J. Phys. Chem. B 105 (2001) 777.
[32] V.G. Mavrantzas, D.N. Theodorou, Macromol. Theory Simul. 9 (2000) 500.
[33] V.A. Harmandaris, V.G. Mavrantzas, D.N. Theodorou, Macromolecules 33 (2000) 8062.
[34] H.C. Andersen, J. Chem. Phys. 72 (1980) 2384.
[35] M. Banaszak, TASK Quart. 5 (2001) 17.
[36] F.F. Abraham, Phys. Rev. Lett. 44 (1980) 463.
[37] F.F. Abraham, W.E. Rudge, D.J. Auerbach, S.W. Koch, Phys. Rev. Lett. 52 (1984) 445.
[38] L. Fritz, D. Hofmann, Polymer 38 (1997) 1035.
[39] W. Brostow, J. Kubát, Phys. Rev. B 47 (1993) 7659.
[40] S. Blonski, W. Brostow, J. Kubát, Phys. Rev. B 49 (1994) 6494.
[41] J. Kubát, M. Rigdahl, Chapter 5 in Ref. [1].
[42] W. Brostow, A.M. Cunha, J. Quintanilla, R. Simoes, Macromol. Theory Simul. 11 (2002) 308.
[43] W. Brostow, K. Hibner, J. Walasek, J. Chem. Phys. 108 (1998) 6484.
[44] W. Brostow, J. Walasek, J. Chem. Phys. 121 (2004) 3272.
[45] W. Brostow, J.A. Hinze, R. Simoes, J. Mater. Res. 19 (2004) 851.
[46] M. Tsige, T. Soddemann, S.B. Rempe, G.S. Grest, J.D. Kress, M.O. Robbins, S.W. Sides, M.J. Stevens, E. Webb III, J. Chem. Phys. 118 (2002) 5132.
[47] S.W. Sides, J. Curro, G.S. Grest, M.J. Stevens, T. Soddemann, A. Habenschuss, J.D. Londono, Macromolecules 35 (2002) 6455.
[48] R. Auhl, R. Everaers, G.S. Grest, K. Kremer, S.J. Plimpton, J. Chem. Phys. 119 (2003) 12718.

[49] J. Rottler, M.O. Robbins, Phys. Rev. E 64 (2001) 051801.
[50] J. Rottler, S. Barsky, M.O. Robbins, Phys. Rev. Lett. 89 (2002) 148304.
[51] J. Rottler, M.O. Robbins, Phys. Rev. E 68 (2003) 011801.
[52] P.J. Flory, Statistical Mechanics of Chain Molecules, Wiley Interscience, New York, 1969.
[53] W.F. van Gunsteren, in: D.G. Truhlar (Ed.), Mathematical Frontiers in Computational Chemical Physics, Springer, New York, 1988.
[54] V. Mom, J. Comput. Chem. 2 (1981) 446.
[55] W. Brostow, A.M. Cunha, R. Simoes, Mater. Res. Innovat. 7 (2003) 19.
[56] W. Brostow, R.P. Singh, in: J. Kroschwitz (Ed.), Encyclopedia of Polymer Science and Technology, Wiley, New York, 2004.
[57] W. Brostow, B. Bujard, P.E. Cassidy, H.E. Hagg, P.E. Montemartini, Mater. Res. Innovat. 6 (2002) 7.
[58] W. Brostow, G. Damarla, J. Howe, D. Pietkiewicz, e-Polymers no. 025, 2004.
[59] R. Simoes, A.M. Cunha, W. Brostow, e-Polymers no. 067, 2004.
[60] W. Brostow, Chapter 10 in Ref. [1].